



The Steady-State ALTADENA RASER Generates Continuous NMR Signals**

Jing Yang,^[a] Peng Wang,^[a] Jan G. Korvink,^[a] Jürgen J. Brandner,^[a] and Sören Lehmkuhl^{*[a]}

A RASER (Radio Amplification by Stimulated Emission of Radiation) facilitates the study of nonlinear phenomena, as well as the determination of NMR parameters with high precision. To achieve maximum sensitivity in the desired operating mode, it is crucial to control the RASER over long periods of time. So far, this was only possible at ultra-low magnetic fields. Here, we introduce a way to control the operating regime of a RASER at a magnetic field of 1.45 T. We employ a continuous-flow RASER, pumped by PHIP (ParaHydrogen Induced Polarization). The hydrogenation of vinyl acetate (VA) with parahydrogen pro-

vides the required negative polarization on the methyl group of the product ethyl acetate (EA). The protons within the methyl group, separated by a 7 Hz J-coupling, are RASER active. This system demonstrates five RASER phenomena: inequivalent and equivalent amplitudes in the “normal NMR mode”, period doublings, frequency combs, and chaos. The experiments match with simulations based on a theoretical model of two nonlinear-coupled RASER modes. We predict the RASER regime at set conditions and visualize the prediction in a bifurcation diagram.

NMR is a versatile and powerful analytical tool in many fields, such as chemistry, biology, pharmacy, and beyond. However, the resolution of any NMR experiment is still limited by the transverse relaxation time T_2 . In this way, any NMR experiment has a minimum natural linewidth, and higher frequency resolution can only be gained at low speed through signal averaging. This limitation can be overcome by a RASER with sub-mHz NMR resolution.^[1]

Additionally, a RASER can be used to study nonlinear phenomena in coupled spin systems,^[2,3] or to transfer polarization to molecules-of-interest (e.g. amino acids) using a PRINOE^[4,5] (Para-hydrogen and RASER Induced Nuclear Overhauser Effect).

A RASER is driven by spontaneous emission of radiation, and therefore does not require external RF excitation.^[1] To operate a RASER, as for the LASER (Light Amplification by Stimulated Emission of Radiation), a population inversion is required. This can be generated for example by hyperpolarization methods. The most common hyperpolarization methods are Spin-Exchange Optical Pumping (SEOP),^[6,7] Dynamic Nuclear Polarization (DNP)^[8–11] and Parahydrogen Induced Polarization

(PHIP).^[12–14] RASERs have been demonstrated with all these techniques: previous work has shown ³He and ¹²⁹Xe RASERs operating with SEOP.^[15] ¹H,^[16–18] ¹⁷O,^[19] and ²⁷Al^[20] RASERs have been shown pumped by DNP. However, SEOP and DNP are currently mostly limited to single-mode operation, and require sophisticated equipment.^[11,21]

With parahydrogen fueled RASERs, various new use-cases were unveiled in recent years, all based on RASERs with multiple frequencies. These included a chemical reaction tracked by a ¹³C RASER,^[22] the study of nonlinear phenomena,^[2,3] and background-free NMR,^[23–25] reaching a frequency resolution below the mHz regime.^[1] Additionally, by introducing magnetic field gradients, RASER modes were used to encode spatial information (RASER MRI).^[26]

Despite all these advantages, a parahydrogen fueled RASER operating at a high magnetic field is burdened by the parahydrogen pumping itself. Parahydrogen bubbles formed in a solution generate susceptibility artifacts that broaden the RASER signals.^[27] Turning off the pumping during acquisition alleviates this problem, but limits RASER signals to bursts that only last until the polarization is depleted.^[2,26] Additionally, over the course of a RASER burst, it passes through different operating regimes and features different types of nonlinear phenomena due to the decaying polarization.^[2]

In this work, we introduce a steady-state RASER operating in different regimes. With two nonlinear-coupled RASER modes, we demonstrate: a starting RASER, the “normal NMR” RASER, a RASER dominated by frequency combs, a RASER dominated by period doublings, and a chaotic RASER (Figure 1a). To obtain the steady-state RASER, highly-polarized ethyl acetate (EA) is continuously supplied to the NMR magnet (Figure 1b). Continuous flow reactors for parahydrogen applications can avoid susceptibility artifacts caused by bubbles and continuously generate a highly polarized liquid.^[28–31] The hyperpolarized EA is generated within a tube-in-tube reactor^[31,32] by hydrogenating vinyl acetate (VA) with parahydrogen (Figure 1c).

[a] J. Yang, P. Wang, Prof. Dr. J. G. Korvink, Prof. Dr. J. J. Brandner, Dr. S. Lehmkuhl
 Institute of Microstructure Technology
 Karlsruhe Institute of Technology
 76344 Eggenstein-Leopoldshafen (Germany)
 E-mail: soeren.lehmkuhl@kit.edu

[**] ALTADENA: Adiabatic Longitudinal Transport After Dissociation Engenders Nuclear Alignment; RASER: Radio-frequency Amplification by Stimulated Emission of Radiation.

Supporting information for this article is available on the WWW under <https://doi.org/10.1002/cphc.202300204>

© 2023 The Authors. ChemPhysChem published by Wiley-VCH GmbH. This is an open access article under the terms of the Creative Commons Attribution Non-Commercial NoDerivs License, which permits use and distribution in any medium, provided the original work is properly cited, the use is non-commercial and no modifications or adaptations are made.

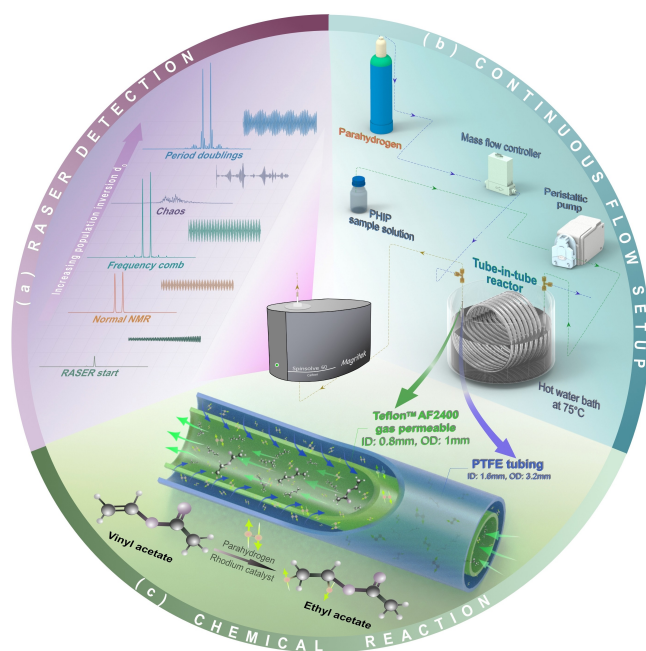


Figure 1. Controlling and monitoring a continuous flow RASER pumped by parahydrogen. (a) Five different ^1H RASER signals in different operating regimes acquired in a 62 MHz benchtop NMR spectrometer. (b) Continuous flow setup to detect steady-state RASER signals. (c) Tube-in-tube reactor containing the PHIP solution (green arrows), where vinyl acetate (VA) is hydrogenated to ethyl acetate (EA) using parahydrogen in countercurrent flow (blue arrows).

A convenient alternative to hydrogenative PHIP is SABRE^[14] (Signal Amplification By Reversible Exchange), which allows for repetitive polarization of the same solution.^[33] However, the polarizations at high concentrations is often lower than in hydrogenative PHIP.^[3,24] Therefore, a hydrogenation reaction is chosen as a model system to access higher population inversions, and with it a broader range of RASER regimes.

In this work, VA is hydrogenated with parahydrogen in a tube-in-tube reactor at the earth's magnetic field with detection at 1.45 T, and thus under ALTADENA^[34] conditions (ALTADENA = Adiabatic Longitudinal Transport After Dissociation Engenders Nuclear Alignment). Hydrogenation under PASADENA conditions^[24] is possible with this setup for example by adding a coil to generate a higher magnetic field around the reactor (PASADENA = Parahydrogen And Synthesis Allow Dramatically Enhanced Nuclear Alignment).

However, ALTADENA is ideal to observe different RASER regimes: we obtain an antiphase ^1H spectrum of the hydrogenation product EA, featuring a positively polarized ethyl group, and a negatively polarized methyl group (Figure 2). The triplet of the methyl group (highlighted in green) can fuel a RASER, as the negative polarization constitutes a population inversion. If the population inversion is high enough, the RASER threshold d_{th} is surpassed and a RASER initiates.^[3] The triplet entails three potential RASER modes $d_{0,\mu}$ ($\mu = 1, 2, 3$) separated by a 7.10 Hz J-coupling. Only two of these modes are RASER active, as the mode with the smallest polarization does not surpass the

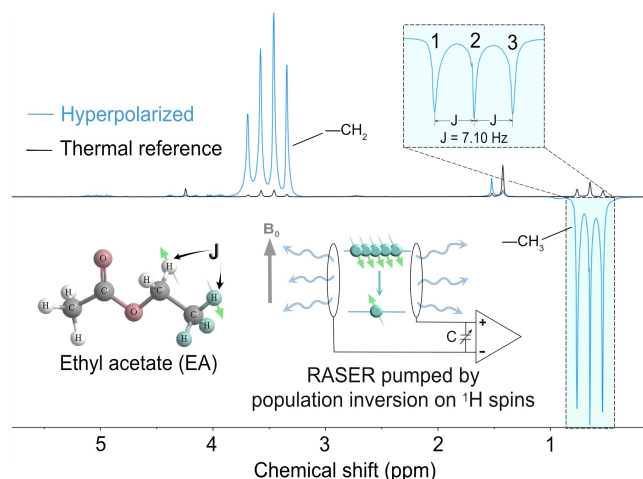


Figure 2. ^1H NMR spectrum of hyperpolarized EA at 1.45 T (blue) compared to a thermal reference spectrum recorded at 1.45 T (grey). The methyl group (highlighted in cyan) is negatively polarized and its resonances can therefore be RASER active. The two modes with the highest intensity (the middle and right mode) surpass the RASER threshold, yielding the two RASER active modes shown in Figure 3. Details on the RASER active modes and the threshold can be found in the Supporting Information.

RASER threshold, but can fuel the other modes as described previously.^[24]

We recorded a series of ^1H RASER signals at 1.45 T under continuous flow conditions (Figure 3, left column). To access different operating regimes, we varied the pressure difference ΔP between the gas and the liquid phase in the tube-in-tube reactor. The higher gas uptake efficiency increased the conversion of the hydrogenation reaction, and therefore, the amount of hyperpolarized EA. This enabled quantitative control over the pumping of the RASER, with the amount of population inversion d_0 reaching the magnet given by Equation (1):

$$d_0 = N_A \cdot V_s \cdot c \cdot P_H \quad (1)$$

where N_A is Avogadro's number, V_s is the sensitive volume of the NMR magnet, c is the concentration, and P_H is polarization of the RASER active ^1H spins.

This pumping d_0 can sustain a steady-state RASER. The steady-state population inversion during an active RASER can be measured by applying a 90° pulse. The resulting FID contains the polarization of both the RASER active modes, as well as modes that are below the RASER threshold, or positively polarized, such as the third resonance of the methyl group, or the ethyl group of EA, respectively (for details, see the Supporting Information). After a 90° excitation pulse, the RASER starts again (Figure 3a), illustrating the competition between two RASER active lines at the initial stage of RASER formation (Figure 3b). The RASER spectrum at 10–15 s shows the two RASER active modes separated by their J-coupling, and with different signal intensities, as one mode is polarized higher and therefore extends further above the RASER threshold. At $t > 20$ s, the RASER signal reaches a steady state.

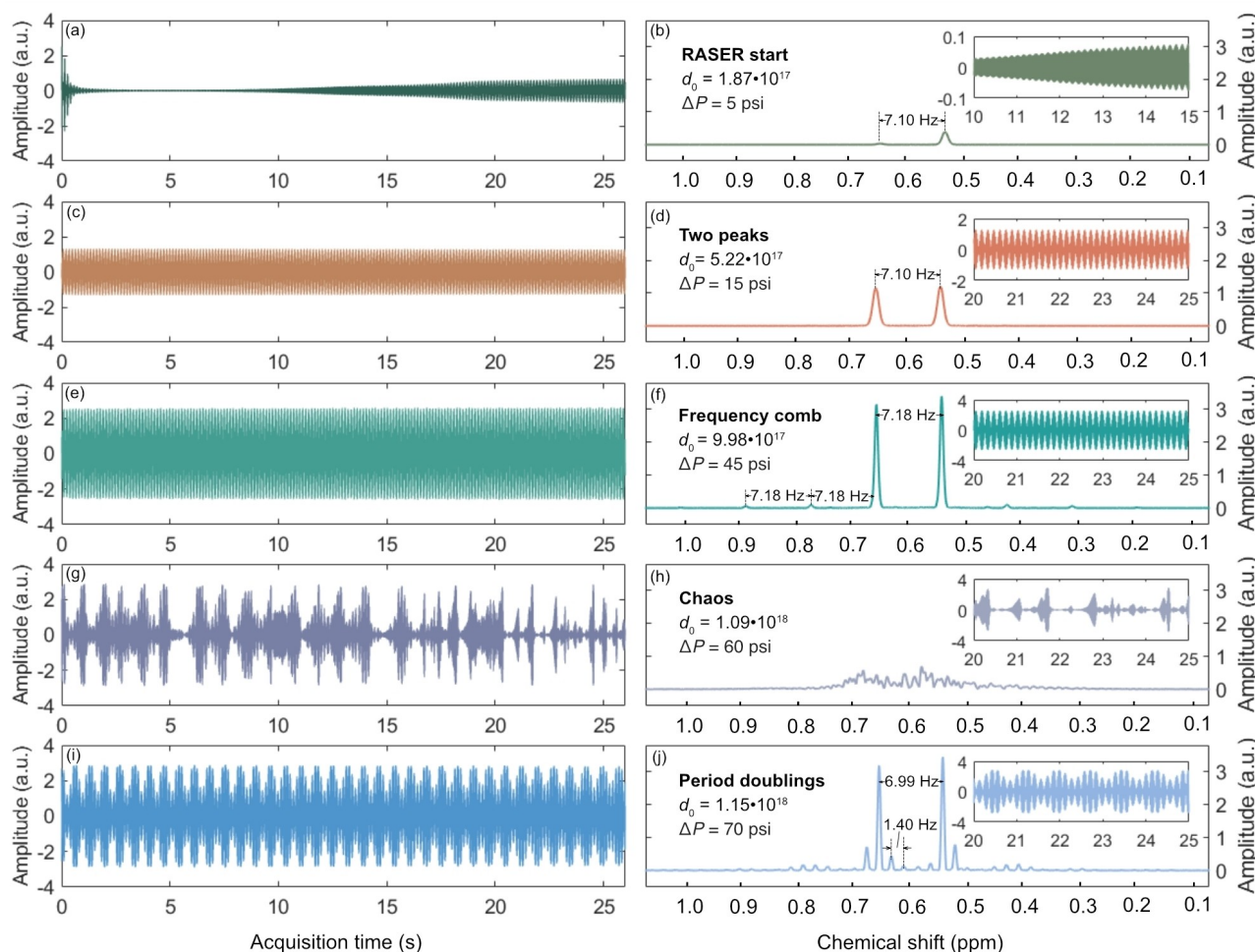


Figure 3. Continuously pumped RASERS of hyperpolarized EA. Left column: ^1H RASER signals stemming from the two RASER active modes introduced in Figure 2. Right column: Corresponding Fourier transformed spectra of selected time slices (shown in the insets). The spectra show different RASER regimes depending on the pumping d_0 . (b) starting RASER, (d) the “normal NMR” mode with two peaks, (f) frequency comb, (h) chaos, and (j) period doublings. The flow rate was set to 4 mL/min in all experiments as a compromise between residence time in the reactor and transport time to the magnet.

By increasing the population inversion to $d_0 = 5.22 \cdot 10^{17}$, a RASER with almost equal intensities on both modes is obtained (Figure 3c). This regime is a convenient choice to measure the J-coupling precisely. Here, the measured frequency difference of 7.10 ± 0.01 Hz is equal to the J-coupling measured for thermally polarized and hyperpolarized EA (Figure 2 and Figure 3d).

With an even higher population inversion level ($d_0 = 9.98 \cdot 10^{17}$), the spectrum features a frequency comb with its two main peaks separated by distance of 7.18 Hz in the middle and side bands, with the same frequency distance (Figure 3f). In this case, the measured frequency difference does not reflect the J-coupling anymore due to frequency shifts, a typical phenomenon in nonlinear systems.

At a pumping of $d_0 = 1.09 \cdot 10^{18}$, the signal features irregular beats (Figure 3g), and the corresponding spectrum is characterized by a continuum of frequencies (Figure 3h). This noise-like spectrum is generated by a multitude of period doubling processes^[26], and is a strong indicator that the system has entered the chaotic regime. The long-term observation of this regime underlines the theoretical prediction that a chaotic

regime can be accessed with a RASER. Previous studies were able to access this regime, but only for a brief moment (< 1 s) due to the changing population inversion within an acquired RASER burst, and the narrow window of the chaotic regime.^[2]

At an even higher d_0 , the RASER enters a regime characterized by a periodic beat pattern (Figure 3i). The corresponding spectrum is an even frequency comb with multiple period doubling processes, where consecutive peaks are separated by 1.40 Hz, and the two main peaks by 6.99 Hz (Figure 3j).

To complement the experimental results, we simulated RASER signals based on the equations introduced by Appelt et al.^[3] For the simulations, two non-linearly coupled RASER modes with a frequency difference $\Delta\nu = 7.0$ Hz are assumed, matching the two RASER active modes from the experiments (see Supporting Information for details on the simulations). The spectra are collected in a bifurcation diagram (Figure 4a), often used to visualize nonlinear chaotic maps like the logistic map.^[35–37] The predicted RASER spectra in the bifurcation diagram match with the experimental results. Depending on d_0 ,

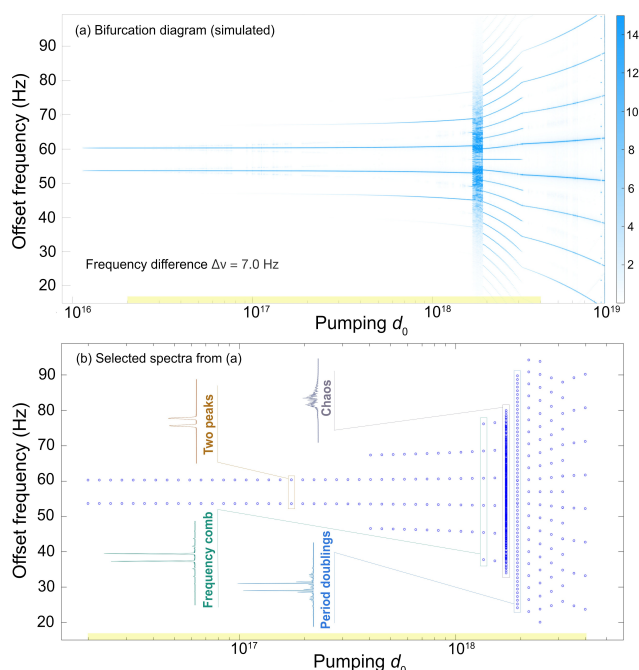


Figure 4. Simulated spectra of two continuously pumped RASER modes separated by 7 Hz at different pumping rates d_0 . In (a), the signal amplitudes are highlighted in a blue color, while (b) depicts the peaks of 45 spectra (only peaks $> 5\%$ of the maximum intensity) in the range of $d_0 \in [2 \cdot 10^{16}, 4 \cdot 10^{18}]$ (highlighted on the pumping axis d_0). With increasing d_0 , all RASER regimes appear in the same sequence as for the experiments shown in Figure 3: two peaks, frequency comb, chaos, and period doublings.

they feature the same regimes: two peaks, frequency combs, period doublings, and chaos (Figure 4b).

The increase of $\Delta\nu$ with increasing d_0 due to frequency shifts, and the reduced $\Delta\nu$ right after the chaotic regime, match the experimental findings. However, global shifts generated for example by distant dipolar fields,^[17,38–40] or external magnetic field fluctuations,^[11] are not included in the simulation as there are several correction algorithms in post processing.^[1,31] The model is thus kept as simple as possible. Therefore, the model slightly deviates from the experimental results as it neglects other polarized spins in the resonator, and the loss of population inversion by polarized material flowing out of the NMR magnet.

In summary, we were able to record a series of steady-state ^1H RASER signals at 1.45 T. Complete control over long periods of time is achieved by using a tube-in-tube reactor. Within the reactor, a highly polarized liquid is continuously generated by hydrogenation of VA with parahydrogen. The resulting highly-polarized product EA pumps the RASER. Depending on the amount of pumping d_0 used for each measurement, we could access different nonlinear RASER regimes. The regimes include situations with two normal NMR resonances, with inequivalent and equivalent amplitudes, frequency combs, period doublings, and chaos. Finally, the observed regimes are matched with simulations based on a two-mode RASER model. The results of the simulation are visualized in a bifurcation diagram. In this way, the operating regime of a RASER can be predicted, to be

able to choose between NMR precision measurements, and the study of nonlinear phenomena.

Experimental Section

Chemical Sample Preparation

All PHIP sample solutions were prepared under inert gas conditions. Each solution contained 400 mmol/l vinyl acetate (VA) and 4.0 mmol/l $[\text{Rh}(\text{dppb})(\text{COD})]\text{BF}_4$ in methanol- d_4 . The deuterated methanol was degassed by three freeze-pump-thaw cycles using a bath of liquid nitrogen and argon. All other chemicals were purchased from Sigma-Aldrich and used without further purification (VA: CAS number: 108-05-4, Sigma-Aldrich, 100 mL; [1,4-Bis-(diphenylphosphino)-butan]-(1,5-cyclooctadien)-rhodium(I)-tetrafluoroborat: CAS number: 79255-71-3, Sigma-Aldrich, 500MG). A parahydrogen fraction of 98% was reached using a commercial helium compressor at 23 K (Advanced Research System, Model ARS-4HW).

Continuous Flow Setup for PHIP Hyperpolarization of Ethyl Acetate (EA)

The main parts of the continuous flow experimental setup are: a mass flow controller for parahydrogen gas, a peristaltic pump (LongerPump BT100-2J) for pumping the PHIP sample solution, two back pressure regulators for control the pressure applied in gas and liquid phase, and a tube-in-tube gas-liquid reactor that introduces the parahydrogen into the solution for the PHIP hyperpolarization.

The tube-in-tube gas-liquid reactor consists of an outer PTFE tubing (ID: 1.6 mm, OD: 3.2 mm) with an inserted inner tubing (TeflonTM AF 2400, ID: 0.8 mm, OD: 1 mm). The inner tubing is a semi-permeable membrane with high gas permeability. It allows for gas transfer from one side to according to the pressure difference. The inner and outer tubing have an overlapped length of 1.5 m to achieve a high contacting area. The liquid PHIP solution and the gaseous parahydrogen flow in opposite directions in the outer and inner tubing. To increase the conversion of the hydrogenation reaction, the tube-in-tube contactor is wrapped into a compact winding, and immersed in a hot water bath at 75 °C. To stop the reaction after the reactor and to improve the quality of the spectra, we placed an ice water bath immediately after the tube-in-tube contactor to cool down the sample solution before NMR signal acquisition.

To ensure that the pressure difference ΔP is the only experimental variable, we chose a constant flow rate of 4 mL/min for all experiments. The flow rate of the sample solution affects both the residence time in the reactor as well as the transport time until detection. If varied, the altered conversion of the hydrogenation reaction and the relaxation losses would change the provided pumping of polarization d_0 .

Processing of the Recorded RASER Signals

To obtain RASER spectra of a five-second time slice, a Hamming filter was applied to the RASER signal to suppress Sinc wiggles. The sliced time domain was zero-filled with twice the signal length both before and after the signal. The final RASER spectra were obtained after a Fast Fourier Transform (FFT) and displayed in the absolute mode. In this way, the five RASER spectra in Figure 3 (right column) are obtained. The corresponding time slices are depicted in the insets.

To obtain spectra for longer time slices, a correction for the magnetic field drift as in TomHon et al.^[31] or Nelson et al.^[22] or for magnetic field fluctuations as in Suefke et al.^[1] would be required. However, five seconds of RASER signal are more than enough to analyze the spectral features in each RASER regime. Furthermore, while the precision at which a frequency difference is detected increases with longer measurement times, this is not necessarily true for the accuracy of the determined J-coupling, which depend on the impact of the nonlinear effects.

Acknowledgements

Research reported in this publication was supported by the German Research Foundation (DFG) under the Grant Agreement No. BR 4175/5-1. Furthermore, funding was provided by the Federal Ministry of Education and Research (BMBF) and the Baden-Württemberg Ministry of Science as part of the Excellence Strategy of the German Federal and State Governments. S. L. is additionally supported by a YIG-Prep-Pro scholarship from KIT, and J. G. K. by the ERC Synergy Grant 951451 (HiSCORE), the DFG via 389084717 (ScreemR), and together with J. J. B., by the DFG CRC1527 (HyPERION). Open Access funding enabled and organized by Projekt DEAL.

Conflict of Interests

The authors declare no conflict of interest.

Data Availability Statement

The data that support the findings of this study are available from the corresponding author upon reasonable request.

Keywords: hyperpolarization · NMR spectroscopy · nonlinear dynamics · parahydrogen · RASER

- [1] M. Suefke, S. Lehmkuhl, A. Liebisch, B. Blümich, S. Appelt, *Nat. Phys.* **2017**, *13*, 568–572.
- [2] S. Appelt, S. Lehmkuhl, S. Fleischer, B. Joalland, N. M. Ariyasingha, E. Y. Chekmenev, T. Theis, *J. Magn. Reson.* **2021**, *322*, 1–47.
- [3] S. Appelt, A. Kentner, S. Lehmkuhl, B. Blümich, *Prog. Nucl. Magn. Reson. Spectrosc.* **2019**, *114–115*, 1–32.
- [4] O. G. Salnikov, I. A. Trofimov, A. N. Pravdivtsev, K. Them, J. B. Hövener, E. Y. Chekmenev, I. V. Koptuyug, *Anal. Chem.* **2022**, *94*, 15010–15017.
- [5] S. Korchak, L. Kaltschnee, R. Dervisoglu, L. Andreas, C. Griesinger, S. Glögler, *Angew. Chem. Int. Ed.* **2021**, *60*, 20984.
- [6] T. Walker, *Spin-exchange Opt. Pump. noble-gas nuclei. Rev Mod Phys* **1997**, *69*, 629–642.
- [7] G. Navon, Y. Q. Song, T. Room, S. Appelt, E. Taylor, A. Pines, *Science* **1996**, *271*, 1848.
- [8] W. A. Barker, *Rev. Mod. Phys.* **1962**, *34*, 173.

- [9] M. Abraham, M. A. H. McCausland, F. N. H. Robinson, *Phys. Rev. Lett.* **1959**, *2*, 449–451.
- [10] J. H. Ardenkjaer-Larsen, *J. Magn. Reson.* **2016**, *264*, 3–12.
- [11] A. C. Pinon, A. Capozzi, J. H. Ardenkjaer-Larsen, *Magn. Reson. Mater. Phys. Biol. Med.* **2021**, *34*, 5–23.
- [12] C. R. Bowers, D. P. Weitekamp, *Phys. Rev. Lett.* **1986**, *57*, 2645.
- [13] C. R. Bowers, D. P. Weitekamp, *J. Am. Chem. Soc.* **1987**, *109*, 5541–5542.
- [14] R. W. Adams, J. A. Aguilar, K. D. Atkinson, M. J. Cowley, P. I. P. Elliott, S. B. Duckett, G. G. R. Green, I. G. Khazal, J. López-Serrano, D. C. Williamson, *Science* **2009**, *323*, 1708–1711.
- [15] T. E. Chupp, R. J. Hoare, R. L. Walsworth, B. Wu, *Phys. Rev. Lett.* **1994**, *72*, 2363–2366.
- [16] H.-Y. Chen, Y. Lee, S. Bowen, C. Hilty, *J. Magn. Reson.* **2011**, *208*, 204–209.
- [17] N. Bloembergen, R. V. Pound, *Phys. Rev.* **1954**, *95*, 8.
- [18] E. M. M. Weber, D. Kurzbach, D. Abergl, *Phys. Chem. Chem. Phys.* **2019**, *21*, 21278–21286.
- [19] M. A. Hope, S. Björgvinsdóttir, C. P. Grey, L. Emsley, *J. Phys. Chem. Lett.* **2021**, *12*, 345–349.
- [20] P. Bösigler, E. Brun, D. Meier, *Phys. Rev. Lett.* **1977**, *38*, 602.
- [21] J. R. Birchall, P. Nikolaou, A. M. Coffey, B. E. Kidd, M. Murphy, M. Molway, L. B. Bales, B. M. Goodson, R. K. Irwin, M. J. Barlow, *Anal. Chem.* **2020**, *92*, 4309–4316.
- [22] C. Nelson, A. B. Schmidt, I. Adelabu, S. Nantogma, V. G. Kiselev, A. Abdurraheem, H. de Maissin, S. Lehmkuhl, S. Appelt, T. Theis, E. Y. Chekmenev, *Angew. Chem. Int. Ed.* **2023**, *62*, e202215678.
- [23] B. Joalland, T. Theis, S. Appelt, E. Y. Chekmenev, *Angew. Chem. Int. Ed.* **2021**, *60*, 26298–26302.
- [24] B. Joalland, N. M. Ariyasingha, S. Lehmkuhl, T. Theis, S. Appelt, E. Y. Chekmenev, *Angew. Chem. Int. Ed.* **2020**, *59*, 8654.
- [25] A. N. Pravdivtsev, F. D. Sönnichsen, J. B. Hövener, *ChemPhysChem* **2020**, *21*, 667–672.
- [26] S. Lehmkuhl, S. Fleischer, L. Lohmann, M. S. Rosen, E. Y. Chekmenev, A. Adams, T. Theis, S. Appelt, *Sci. Adv.* **2022**, *8*, eabp8483.
- [27] A. N. Pravdivtsev, F. D. Sönnichsen, J. B. Hövener, *ChemPhysChem* **2020**, *21*, 667–672.
- [28] S. Lehmkuhl, M. Wiese, L. Schubert, M. Held, M. Küppers, M. Wessling, B. Blümich, *J. Magn. Reson.* **2018**, *291*, 8–13.
- [29] L. Bordonali, N. Nordin, E. Fuhrer, N. Mackinnon, J. G. Korvink, *Lab Chip* **2019**, *19*, 503–512.
- [30] J. Eills, W. Hale, M. Sharma, M. Rossetto, M. H. Levitt, M. Utz, *J. Am. Chem. Soc.* **2019**, *141*, 9955–9963.
- [31] P. M. TomHon, S. Han, S. Lehmkuhl, S. Appelt, E. Y. Chekmenev, M. Abolhasani, T. Theis, *ChemPhysChem* **2021**, *22*, 2526–2534.
- [32] W. G. Hale, T. Y. Zhao, D. Choi, M. Ferrer, B. Song, H. Zhao, H. E. Hagelin-Weaver, C. R. Bowers, *ChemPhysChem* **2021**, *22*, 822–827.
- [33] J. B. Hövener, N. Schwaderlapp, T. Lickert, S. B. Duckett, R. E. Mewis, L. A. R. Highton, S. M. Kenny, G. G. R. Green, D. Leibfritz, J. G. Korvink, J. Hennig, D. Von Elverfeldt, *Nat. Commun.* **2013**, *4*, DOI 10.1038/ncomms3946.
- [34] M. G. Pravica, D. P. Weitekamp, *Chem. Phys. Lett.* **1988**, *145*, 255–258.
- [35] M. J. Feigenbaum, *J. Stat. Phys.* **1978**, *19*, 25–52.
- [36] A. Y. Okulov, A. N. Oraevsky, *J. Opt. Soc. Am. B* **1986**, *3*, 741–746.
- [37] R. B. Naik, U. Singh, *Ann. Data Sci.* **2022**, DOI 10.1007/s40745-021-00364-7.
- [38] N. Bloembergen, R. V. Pound, *Phys. Rev.* **1954**, *95*, 8.
- [39] A. Vlassenbroek, J. Jeener, P. Broekaert, *J. Chem. Phys.* **1995**, *103*, 5886–5897.
- [40] H. Desvaux, *Prog. Nucl. Magn. Reson. Spectrosc.* **2013**, *70*, 50–71.

Manuscript received: March 22, 2023

Revised manuscript received: April 29, 2023

Accepted manuscript online: May 14, 2023

Version of record online: June 12, 2023